



## Protective effects of boric acid possessing antioxidant and cytoprotective properties against cyclophosphamide-induced liver damage in rats: A histopathological and stereological study

Elfide Gizem Bakirhan<sup>1</sup>, Ebru Annac<sup>1</sup>, Elif Merve Betül Yanilmaz<sup>2</sup>, Nurhan Tirasci<sup>2</sup>

<sup>1</sup> Department of Histology and Embryology, Faculty of Medicine, Adiyaman University, Adiyaman, Türkiye

<sup>2</sup> Experimental Animal Production Application and Research Center, Adiyaman University, Adiyaman, Türkiye

Received: 08.06.2025; Revised: 01.08.2025; Accepted: 04.08.2025

### Abstract

**Objective:** Our study was conducted to investigate the potential protective activities of boric acid (BA), which exhibits antioxidant and protective properties against cyclophosphamide (CP)-induced liver injury in rats, using histopathological and stereological methods.

**Methods:** Twelve-week-old rats were randomly assigned to one of four groups of eight animals each: Control (Cont: receiving 1 ml tap water by oral gavage for 7 days), CP (a single intraperitoneal (i.p.) dose of 150 mg/kg, BA (15 mg/kg/day, orally for 7 days), and CP+BA (a single dose of 150 mg/kg CP i.p., plus 15 mg/kg/day BA by oral gavage for 7 days). At the end of the experiment, liver tissues were collected after anesthesia and decapitation. Total liver and sinusoidal volumes were estimated using the Cavalieri method. Hematoxylin-eosin, Masson trichrome, and periodic acid-Schiff (PAS) staining were applied for histopathological evaluations.

**Results:** Stereological analysis revealed a statistically significant increase in total liver volume in the CP group compared to the Cont ( $p=0.004$ ) and CP+BA groups ( $p=0.045$ ). Sinusoidal volume was also significantly higher in the CP group compared to the Cont ( $p=0.001$ ) and CP+BA groups ( $p=0.037$ ). Histopathological examination revealed impaired hepatic architecture, hepatocyte degeneration, and increased sinusoidal dilatation and mast cell density in the CP group. In contrast, a partially preserved liver histology with reduced degeneration was observed in the CP+BA group.

**Conclusion:** BA treatment exhibits a partial hepatoprotective effect against CP-induced liver injury, as shown by both the stereological and histopathological analyses. The study findings indicate the hepatoprotective potential of BA treatment and suggest that it represents a promising candidate for therapeutic use.

**Keywords:** Boric acid; Cyclophosphamide; Liver damage

DOI: 10.5798/dicletip.1784951

**Correspondence / Yazışma Adresi:** Elfide Gizem Bakirhan, Department of Histology and Embryology, Faculty of Medicine, Adiyaman University, Adiyaman, Türkiye e-mail: elfide.gzm@gmail.com

## Sıçanlarda siklofosfamid kaynaklı karaciğer hasarına karşı antioksidan ve sitoprotektif özelliklere sahip borik asidin koruyucu etkileri: Histopatolojik ve stereolojik bir çalışma

### Öz

**Amaç:** Çalışmamızda, histopatolojik ve stereolojik yöntemler kullanarak sıçanlarda siklofosfamid (CP) kaynaklı karaciğer hasarına karşı antioksidan ve koruyucu özelliklere sahip olan borik asidin (BA) potansiyel koruyucu rolünü değerlendirmeyi amaçlamaktadır.

**Yöntemler:** Çalışmamızda 12 haftalık sıçanı rastgele dört gruba ayrıldı (n=8): Kontrol (Cont: 7 gün boyunca oral gavaj ile 1ml çeşme suyu), CP (tek doz 150 mg/kg, i.p.), BA (15 mg/kg/gün, 7 gün boyunca oral) ve CP+BA (tek doz 150 mg/kg, i.p CP, 7 gün boyunca oral gavaj ile 15 mg/kg/gün BA). Deney sonunda, anestezi ve dekapitasyonun ardından karaciğer dokuları toplandı. Toplam karaciğer ve sinüzoidal hacimler Cavalieri yöntemi kullanılarak tahmin edildi. Histopatolojik değerlendirmeler için hematoksilin-Eozin, Masson trikromu ve PAS boyamalar yapıldı.

**Bulgular:** Stereolojik analiz, CP grubunda Cont (p=0.004) ve CP+BA (p=0.045) gruplarına kıyasla toplam karaciğer hacminde istatistiksel olarak anlamlı bir artış olduğu gözlemlendi. Sinüzoidal hacim de CP grubunda Cont (p=0.001) ve CP+BA (p=0.037) gruplarına kıyasla anlamlı bir şekilde arttı görüldü. Histopatolojik olarak, CP grubunda bozulmuş hepatik mimari, hepatosit dejenerasyonu ve artmış sinüzoidal dilatasyon ve mast hücre yoğunluğu görüldü. Buna karşılık, CP+BA grubunda dejenerasyonun azaldığı kısmen korunmuş karaciğer histolojisi görüldü.

**Sonuç:** BA tedavisi, hem stereolojik hem de histopatolojik analizlerle gösterildiği üzere, CP kaynaklı karaciğer hasarına karşı kısmi hepatoprotektif etki göstermektedir. Çalışmamız, BA tedavisi hepatoprotektif potansiyelini ortaya koymakta ve olası terapötik kullanımı açısından umut verici bir aday olduğunu düşündürmektedir.

**Anahtar kelimeler:** Borik ait; Siklofosfamid; Karaciğer hasarı.

### INTRODUCTION

Cyclophosphamide (CP) is one of the most effective chemotherapeutic agents. CP is an alkylating agent, whose active metabolites acrolein and phosphoramidate mustard are implicated in cell cytotoxicity. These chemically reactive metabolic products cause alkylating effects on DNA cross-links and DNA itself, resulting in cytotoxicity<sup>1</sup>. Due to its direct cytotoxic effect on tumors, CP is used in the treatment of lymphoma, leukemia, and hematological malignancies, as well as various epithelial tumors including breast, ovarian and small cell lung carcinomas<sup>2,3</sup>. However, this cytotoxicity causes numerous side-effects in various tissues<sup>4</sup>. CP is metabolized and excreted in the liver and kidney, and these are therefore among the organs that exhibit the greatest side-effects<sup>5</sup>. Acrolein, produced as a result of the metabolism of CP by the CYP450 enzyme in the liver, reacts with intracellular reduced glutathione (GSH) to produce reactive oxygen

species (ROS) and causes suppression of the antioxidant defense mechanism. This results in focal cell necrosis and apoptosis, leading to general damage in the liver tissue<sup>6-8</sup>. Natural therapeutic agents capable of assisting in the control of reactions to chemotherapy and also of reducing the undesirable side-effects of antineoplastic agents to a minimum are therefore of great medical importance.

Boron or boric acid (BA) is a naturally occurring mineral abundantly present in Türkiye. With its antioxidant, anti-inflammatory and anti-apoptotic effects, BA is widely used in both experimental and clinical applications<sup>9,10</sup>. Studies have suggested that BA increases glutathione stores in the body and prevents oxidative damage by suppressing other ROS<sup>11</sup>.

Our scan of the existing literature revealed no previous stereological study examining the hepatoprotective effect of BA application for reducing liver tissue damage caused by CP. This study hypothesizes that BA, due to its well-

known antioxidant and cytoprotective properties, may alleviate CP-induced hepatotoxicity by reducing oxidative stress and preserving liver tissue integrity. The aim of this research is to evaluate the protective effects of BA against CP-induced liver damage in rats through detailed histopathological and stereological analyses.

## **METHOD**

### **Creation of the experimental model**

Thirty-two female 12-week-old Wistar albino rats weighing 220-250 g were used in this study. All experimental animals were obtained from the Adiyaman University Experimental Animals Center after the receipt of approval from the Adiyaman University experimental animals ethics committee (no. 2024/017 dated 02.05.2024), and all experimental procedures were carried out in the center. Ad libitum access was permitted to standard chow and water, and the animals were housed in rooms with a 12-hour light and 12-hour dark light cycle at a  $22 \pm 20^\circ\text{C}$  room temperature during the experiment. Four groups, each containing eight rats, were established. The groups were formed as follows;

1. Control group (Cont): 1 ml of tap water was applied to the animals in this group by oral gavage on days<sup>1-7</sup>.
2. Cyclophosphamide (CP) group: Animals in this group received a single intraperitoneal (i.p.) injection of 150 mg/kg CP on the first day of the study<sup>12</sup>.
3. CP+BA group: This group received a single i.p. injection of CP (at a dose of 150 mg/kg) on day 1 and BA at a dose of 15 mg/kg via intragastric gavage on days<sup>1-7,13</sup>.
4. Boric acid (BA) group: Animals in this group received 15 mg/kg BA (dissolved in 0.9% NaCl) via intragastric gavage on days<sup>1-7,13</sup>.

The number of animals to be used in our study was determined using the G power program based on the data obtained from published

studies. At the end of the seven-day experimental procedures, all animals were sacrificed by decapitation on day 8 under ketamine (90 mg/kg) and xylazine (10 mg/kg) anesthesia. The liver tissues from all four groups were next removed and placed in 10% formaldehyde for histopathological and stereological examinations.

### **Histological Analyses**

Liver samples collected for histopathological examination were first placed in a 10% formaldehyde solution. Following one-week fixation, routine histological tissue procedures were performed and paraffin blocks were prepared, from which 5-micron-thick sections were taken. These sections were stained with hematoxylin-eosin for histopathological evaluations, Masson trichrome to demonstrate connective tissue density, toluidine blue to demonstrate mast cell density, and periodic acid-Schiff (PAS) to demonstrate glycogen accumulation. Images captured with a Carl Zeiss brand Axiocam ERc5 model digital camera-attached microscope were used in the histopathological evaluations. These procedures were performed in the XXX University Faculty of Medicine histology and embryology department laboratory.

### **Stereological Analyses**

Stereological methods are employed to elicit the quantitative features of three-dimensional structures by means of two-dimensional images. The Cavalieri principle was used for volume calculations in the present study. Paraffin blocks with a thickness of 5  $\mu\text{m}$  were sampled at a rate of 1/15 in line with the systematic random sampling rule. Approximately 10-15 sections were obtained, and these were stained with hematoxylin-eosin (H&E) for visualization under a light microscope. All images were photographed by projection onto a computer screen with a Carl Zeiss Axiocam brand ERc5 model (Carl Zeiss

Microscopy GmbH 07745 Jena, Germany) light microscope with a 10x objective lens and a digital color camera attachment. Liver and sinusoidal volumes were calculated from all the section images using the Cavalieri method. This technique relies on multiplying the surface area of the examined object by the average section thickness. For surface area calculations, regular grid test points (liver and sinusoid) randomly laid over the section images using the point counting method were counted on Image J software (Image Processing and Analysis in JAVA, NIH, USA). After calculating the surface areas, the following formulae were used to determine the volume values;

$$V_{ref} = \sum P_i \times t$$

$$P_i = P(a)$$

$$\sum V = V_1 + V_2 + V_3 + \dots$$

“ $V_{ref}$ ” represents the total or reference volume of the relevant structure; “ $\sum P_i$ ”, the total number of points hitting the cross-sectional surface area; “ $P(a)$ ” the area represented by a point on the dotted area table; “ $t$ ” the average cross-section thickness; and “ $V$ ” the volume value of a palatine tissue section. After applying the same formula for all cross-sections, the total volume values were calculated by adding the volume values. The grid size was determined, and coefficient of error (CE) for one subject and coefficient of variation (CV) for the group were estimated as determined in previous pilot studies<sup>14</sup>.

### Statistical Analysis

SPSS software (SPSS version 21.0; SPSS Inc., Chicago, IL, USA) was employed for statistical analyses. The data were expressed as mean  $\pm$  standard error. Normality (Shapiro-Wilk) and homogeneity tests confirmed that all four groups exhibited normal distribution. One-Way ANOVA and the Tukey test were applied to evaluate intergroup differences.  $p$  values  $<0.05$  were regarded as statistically significant.

## RESULTS

### Stereological Findings

The total liver and sinusoidal volumes of all groups calculated by means of the Cavalieri method are shown in graph form below (Figure 1 A, B).

**Table I:** CE and CV values of stereologically analyzed the total liver and sinusoidal volumes of all groups

Gruplar	Total liver volumes		Sinusoidal volumes	
	CE	CV	CE	CV
Cont	0.07	0.13	0.07	0.15
CP	0.06	0.11	0.06	0.12
CP+BA	0.08	0.14	0.06	0.11
BA	0.06	0.13	0.05	0.13

### Total liver volume findings

The total liver volumes in all four groups calculated using the Cavalieri method were subjected to evaluation. The total liver volume in the CP group increased significantly compared to the Cont group ( $p=0.004$ ). Similarly, the total volumes were lower in the CP+BA and BA groups than in the CP group (respectively  $p=0.045$ ,  $p=0.039$ ). However, no significant difference was observed between the Cont group and the CP+BA group ( $p=0.059$ ). This result shows that BA prevents the increase in liver volume caused by CP (Figure 1 A).

### Total sinusoidal volume findings

The sinusoidal volumes of liver tissues from all four groups were also evaluated using the Cavalieri method. The results revealed that the sinusoidal volume value in the CP group increased significantly compared to the Cont group ( $p=0.001$ ). A statistically significant difference was also observed in the CP+BA group compared to the CP group ( $p=0.037$ ) (Figure 1B). However, no significant differences were determined between the Cont and CP+BA ( $p=0.86$ ). It may therefore be concluded that BA reverses the increase in sinusoidal volume caused by CP.

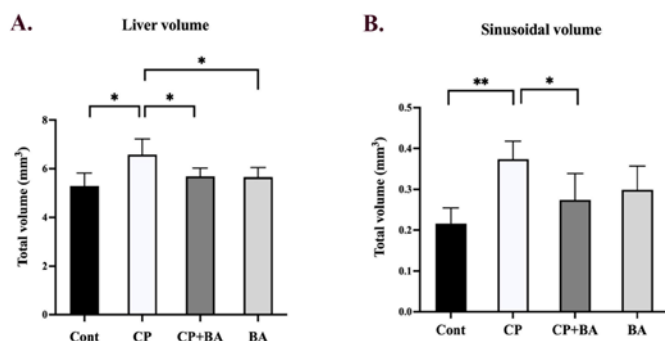


**Figure 1.** Graph showing stereological volumetric analyses in the liver. A. Liver volume, B. Sinusoidal volume. Differences that are statistically significant at the  $p < 0.05$  level are indicated by "\*", and those significant at the  $p < 0.01$  level by "\*\*\*" (mean  $\pm$  SD)

### Light Microscopic Findings

Examination of the H&E-stained sections from the Cont and BA groups revealed that the central vein in the middle of the liver lobule, the hepatocyte cords extending from the central vein to the periphery, and the sinusoids located between these cords were all normal in appearance. The presence of polygonal liver cells was observed. Hepatocyte cytoplasm showed variable acidophilic staining depending on cell activity. The nuclei of these cells were large, round, euchromatic, and centrally located. In addition, some hepatocytes possessed two nuclei and exhibited a normal structure (Figures 2A and 5A). Masson's triple staining method was applied to the tissues from the Cont and BA groups in order to show the density of the connective tissue. Non-dense connective tissue was observed around the cv and in the periportal area (Figures 2B and 5B). Densities were normal in the mast cells in the connective tissue around the vessels in both groups (Figures 2C and 5C). Normal density PAS (+) uptake was observed (Figures 2D and 5D). Examination of the H&E-stained sections from the CP group revealed disruption in the arrangement of the hepatocyte cords formed by hepatocytes around the central vein at low magnification. In addition, the lobule structure

and the borders thereof could not be clearly distinguished. At high magnification of tissues from that group, due to disruption of the cellular integrity of the hepatocytes forming the parenchyma, the connections between the cells were impaired, and their cytoplasmic borders could not be clearly distinguished, their polygonal shapes were lost, and size differences and degenerative changes were determined between the cells. These cells also exhibited a dark pyknotic nucleus in some areas. In addition, partial expansion was observed in the sinusoidal structures (Figure 3A). In the rat liver tissues from the CP group exposed to Masson's triple staining in order to show the connective tissue density, non-dense connective tissue was observed around the central vein and in the periportal area, similarly to the other groups (Figure 3B). The density of mast cells in the connective tissue around the vessels was significantly higher than in the other groups (Figure 3C). An increase in the PAS (+) uptake rate was also observed (Figure 3D). Examination of H&E-stained sections from the CP+BA group revealed a regular structure around the central vein at low magnification in the hepatocytes forming the parenchyma, similarly to the control and BA groups. High-magnification examination of the CP+BA group revealed a normal architecture in the hepatocytes forming the liver parenchyma, with a preserved acidophilic structure. The presence of degenerated hepatocytes persisted, although their density was lower (Figure 4A). Masson's triple staining method revealed a similar connective tissue density around the central vein and in the periportal area to those of the other groups (Figure 4B). Mast cell density was slightly reduced compared to the CP group (Figure 4C). The PAS (+) uptake rate was higher than in the Cont and BA groups (Figure 4D). No inflammation or hemorrhagic findings were observed in the tissues.



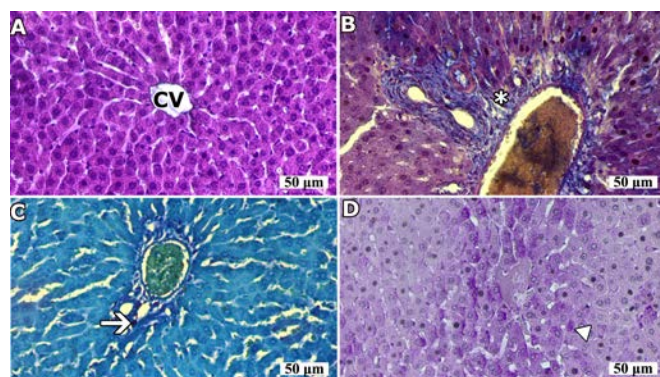


**Figure 2.** Images of the Cont group at x40 objective magnification. (A, H&E staining; B, Masson trichrome staining; C, Toluidine blue staining; D, PAS staining) cv, central vein; star, connective tissue area; arrow, mast cell; arrowhead, PAS (+) cells.

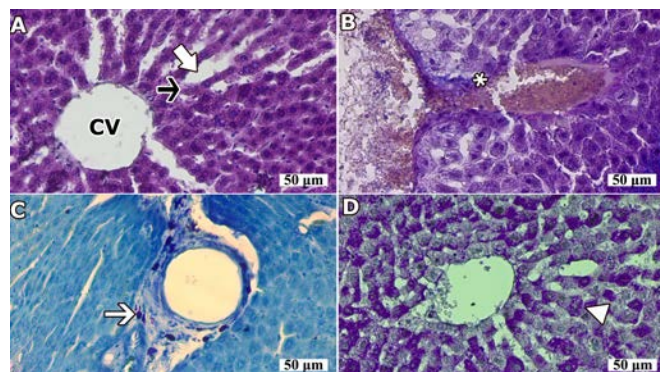


**Figure 3.** Images of the CP group at x40 objective magnification. (A, H&E staining; B, Masson trichrome staining; C, Toluidine blue staining; D, PAS staining) Black arrow, degenerated hepatocyte cells; thick white arrow, dilated sinusoid; cv, central vein; star, connective tissue area; arrow, mast cell; arrowhead, PAS (+) cells.

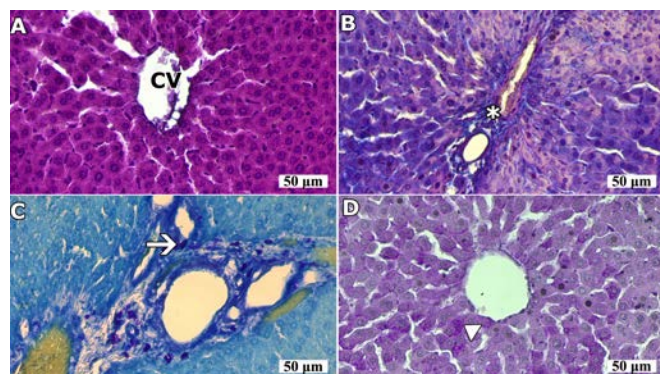


**Figure 4.** Images of the CP+BA group at x40 objective magnification. (A, H&E staining; B, Masson trichrome staining; C, Toluidine blue staining; D, PAS staining) Thin arrow, degenerated hepatocyte cells; cv, central vein; star, connective tissue area; arrow, mast cell; arrowhead, PAS (+) cells

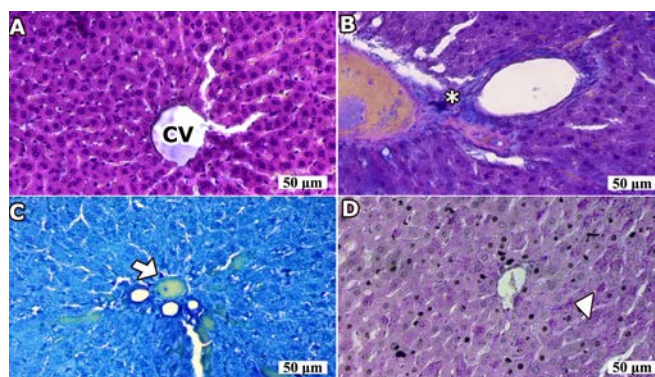


**Figure 5.** Images of BA group at x40 objective magnification. (A, H&E staining; B, Masson trichrome staining; C, Toluidine blue staining; D, PAS staining) cv, central vein; star, connective tissue area; arrow, mast cell; arrowhead, PAS (+) cells.

## DISCUSSION

In this study, the hepatoprotective effects of boric acid (BA) against cyclophosphamide (CP)-induced liver injury were evaluated using histopathological and stereological approaches. CP, a potent chemotherapeutic agent, is known to induce oxidative stress through its metabolites, leading to liver damage characterized by inflammation, hepatocyte degeneration, and tissue architectural disruption. Our findings are consistent with previous reports describing CP-induced liver injury, but offer new insights with unbiased stereological quantification and detailed histopathological assessment.

Previous studies have shown that CP metabolites disrupt the antioxidant balance (including catalase (CAT), superoxide dismutase (SOD), glutathione peroxidase (GSH), and malondialdehyde (MDA) by causing increased free radical production, and this leads to oxidative stress in tissues<sup>15-18</sup>. The histopathological results of this study confirmed that CP causes liver damage, as shown by the impaired arrangement of hepatocyte cords, the disruption of the lobule structure, the degenerative hepatocyte structure, the inability to clearly distinguish their cytoplasmic borders, the presence of

pyknotic nuclei in the cells, and the increase in mast cell density around the vessels and connective tissue. Similarly, the sinusoidal expansions observed histopathologically were also confirmed by the stereological analyses. Those evaluations revealed a significant increase in total liver and sinusoidal volume values compared to the Cont group. This is an expected result considering the processes of sinusoidal dilatation, inflammation, and increase in connective tissue that occur in connection with CP.

In parallel with the results of the present study, Li et al. (2015) applied histopathological methods to evaluate the effects of CP (80 mg/kg) on liver tissue in a S180 carrying mouse model and observed histological changes such as liver congestion, hepatic cord irregularities, and ballooning degeneration on H&E-stained slides. In addition, the decrease in SOD and GSH activities and the increase in MDA those authors observed in their biochemical evaluations may reflect the pathological effects on liver tissue of CP, which causes an imbalance in the antioxidant system in hepatic tissue<sup>19</sup>. Another study observed that CP (80 mg/kg)-induced oxidative stress caused a rise in caspase-3 and NF- $\kappa$ B immunoreactivity in liver tissue, thus increasing apoptotic and inflammatory parameters. In addition, histopathological evaluation revealed changes such as inflammatory cell infiltration, severe congestion, sinusoidal widening, and hemorrhage in liver tissues<sup>18</sup>. Çağlayan et al. (2018) reported that CP (200 mg/kg bw) administration activated the apoptotic and autophagic pathways by enhancing the expression of cysteine aspartate-specific protease-3 (caspase-3) and light chain 3B (LC3B) levels in liver tissue, while at the same time increasing the expression of the oxidative DNA damage marker 8-hydroxy-2'-deoxyguanosine (8-OHdG). In addition, histopathological analysis in that study

confirmed that CP caused hepatic damage, as demonstrated by the presence of hydropic degeneration, coagulation necrosis, mononuclear cell infiltration, and sinusoidal dilatation and hyperemia in hepatocytes<sup>20</sup>. Similar results were also obtained in the current study. It may be concluded that the intensive metabolism of CP by the liver induces hepatic oxidative stress, and that this oxidative stress leads to severe pathologies in liver tissue.

It is essential to investigate different compounds that are capable of reducing the inevitable side-effects of CP on liver tissue. This study investigated the role of BA in preventing CP-induced liver damage. BA reduced the degeneration caused by CP in the liver and prevented CP-induced changes. Stereological examination of total liver and sinusoidal volumes revealed significantly lower volume values in the BA-treated group compared to the CP group. These results show that BA causes a decrease in total liver volume by regulating sinusoidal volume.

Previous studies have also shown that BA exhibits therapeutic effects especially on the liver, one of its target tissues<sup>21,22</sup>. In their study examining the toxic impacts of CP exposure on the rat liver and the protective effects of BA, Cengiz et al. found that BA reduced the previously heightened total oxidant status (TOS), oxidative stress index (OSI) values, and caspase-3 levels caused by CP, while normalizing previously decreased total antioxidant capacity (TAC) levels. Those authors therefore concluded that BA successfully protected the liver against apoptosis and histopathological changes deriving from CP<sup>23</sup>. These findings suggest that beneficial effects of BA are due to its free radical scavenging activity, which disrupts the antioxidant balance in tissues. However, at the cellular signaling level, BA may suppress inflammation by reducing the activation of nuclear factor-kappa B (NF- $\kappa$ B), which plays a

central role in the expression of proinflammatory cytokines. Furthermore, BA may regulate apoptotic pathways by decreasing the expression of proapoptotic markers such as caspase-3 and enhancing antiapoptotic responses. These combined antioxidant, anti-inflammatory, and anti-apoptotic effects may contribute to the overall protective role of BA in liver tissue exposed to chemotherapeutic-induced oxidative stress.

Another study showed that BA was capable of slowing the histological progression of CP-induced hepatotoxicity by significantly reducing the degree of hepatocyte degeneration caused by CP. BA exhibited this hepatotropic effect in the liver by lowering MDA levels and increasing SOD, GSH-Px, and CAT activities in the liver<sup>24</sup>. These findings are consistent with the results of the present study, suggesting that BA can prevent the oxidative stress and damage caused by various toxic substances in liver tissue. In contrast, Gündüz et al. (2023) demonstrated that boric acid did not provide significant protection against acrylamide-induced liver toxicity and did not affect normal TAC<sup>25</sup>. However, it was reported to slightly reduce histopathological damage. These conflicting findings highlight that the hepatoprotective effects of boric acid may be model-dependent and may vary depending on the type, dose, and mechanism of the hepatotoxic agent. Therefore, while boric acid may exhibit protective effects in some models of oxidative stress-induced liver injury, its efficacy appears limited or insufficient in others. In this context, the results highlight the need for further studies to clarify the therapeutic potential of BA across different exposures.

Moreover, one of the distinguishing strengths of this study is the inclusion of unbiased stereological methods in the assessment of CP-induced liver injury and the protective effects of BA. While previous studies relied solely on histopathological or biochemical assessments

(CAT, SOD, GSH, MDA, etc.), the use of stereological volume estimation techniques in this study provided objective, quantitative data on changes in liver and sinusoidal volumes. This approach increased the reliability and scientific rigor of the findings by providing a more sensitive and reproducible assessment of tissue changes. To our knowledge, no studies in the literature have applied stereology to assess both the extent of CP-induced liver injury and the therapeutic effect of BA. Therefore, the inclusion of stereological analysis represents a novel and valuable contribution to the field and may serve as a methodological model for future hepatotoxicity studies. However, a particular limitation of this study is that molecular approaches could not be included. We intend to design more detailed studies including different techniques to elucidate these molecular pathways in future studies.

Nevertheless, while the findings obtained in this study provide valuable insights into the role of mast cells in the relevant pathological processes, certain methodological limitations must also be acknowledged. In particular, the absence of molecular-level analyses and quantitative evaluations of mast cells may be considered a factor that limits the scope of the findings. These shortcomings necessitate caution in the interpretation of the results and underscore the need for future studies that address these aspects, which would contribute to a more comprehensive understanding of the underlying cellular mechanisms.

## CONCLUSION

The results of this study showed that CP application caused structural deterioration in liver tissue, while BA application has been shown to reduce these harmful effects. Stereological analyses showed that BA application prevented CP-induced increases in total liver and sinusoidal volumes. It may therefore be concluded that BA is effective in reducing CP-induced hepatotoxicity and exerts



a significant protective effect on liver tissue. Considering its ability to restore antioxidant parameters and ameliorate histopathological disruptions, BA holds noteworthy translational potential in clinical settings. This research will contribute to the limited number of existing studies aimed at reducing CP-induced liver damage with BA and provides an original examination of the literature, especially in terms of stereological evaluation. However, in order to better understand the full scope of its protective mechanisms and to validate its clinical applicability, further mechanistic studies are warranted. Future research should incorporate molecular and biochemical markers such as the expression of oxidative stress-related genes, pro-inflammatory cytokines, apoptotic regulators, and fibrotic signaling pathways to elucidate the precise intracellular pathways modulated by BA. Moreover, dose-response analyses, pharmacokinetic evaluations, and in vivo molecular imaging may provide critical insights into its bioavailability and systemic effects. These investigations will not only help clarify BA's therapeutic mechanism of action but also determine its feasibility and safety in clinical applications.

**Ethics Committee Approval:** Ethical protocol was approved by Adiyaman University Ethics Committee, approval number (Decision No: 2024/017-08).

**Conflict of Interest:** The authors declare no conflicts of interest.

**Financial Disclosure:** The authors declared this study has received no financial support.

## REFERENCES

1. Asiri YA. Probucol attenuates cyclophosphamide-induced oxidative apoptosis, p53 and Baxsignal expression in rat cardiac tissues. *Oxid Med Cell Longev*. 2010; 3: 308–16.
2. Emadi A, Jones RJ, Brodsky RA. Cyclophosphamide and cancer: golden anniversary. *Nat Rev Clin Oncol*. 2009; 6: 638–47.
3. Şahin F, Deveci E, Aşır F, Albayrak MGB, Özkorkmaz EG. Investigation of the effect of rosmarinic acid on cyclophosphamide-induced gonadal toxicity. *ASM*. 2022; 12: 1-8.
4. Madondo MT, Quinn M, Plebanski M. Low dose cyclophosphamide: Mechanisms of T cell modulation. *Cancer Treat Rev*. 2016; 42: 3–9.
5. Abdelfattah-Hassan A, Shalaby SI, Khater SI, et. al. Panax ginseng is superior to vitamin E as a hepatoprotector against cyclophosphamide-induced liver damage. *Complement Ther Med*. 2019; 46: 95–102.
6. Nuño-Lámbarri N, Domínguez-Pérez M, Baulies-Domenech A, et al. liver cholesterol overload aggravates obstructive cholestasis by inducing oxidative stress and premature death in mice. *Oxid Med Cell Longev*. 2016; 2016: 9895176.
7. Hao H, Xu Y, Chen R, et al. Protective effects of chlorogenic acid against cyclophosphamide induced liver injury in mice. *Biotec Histochem*. 2024; 99: 33–43.
8. Habibi E, Shokrzadeh M, Chabra A, et al. Protective effects of *Origanum vulgare* ethanol extract against cyclophosphamide-induced liver toxicity in mice. *Pharm Biol*. 2015; 53: 10–5.
9. Cengiz M. Boric acid protects against cyclophosphamide-induced oxidative stress and renal damage in rats. *Cell Mol Biol*. 2018; 64: 11–4.
10. Hadrup N, Frederiksen M, Sharma AK. Toxicity of boric acid, borax and other boron containing compounds: A review. *RTP*. 2021; 121:104873.
11. Basbug M, Yildar M, Yaman İ, et al. Effects of boric acid in an experimental rat model of hepatic ischemia-reperfusion injury. *Acta Med*. 2015; 31:1067-1073.
12. Abogresha NM, Mohammed SS, Hosny MM, et al. Diosmin mitigates cyclophosphamide induced premature ovarian insufficiency in rat model. *Int J Mol Sci*. 2021; 22: 1–20.
13. Çolak S, Koc K, Yıldırım S, Geyikoğlu F. Effects of boric acid on ovarian tissue damage caused by experimental ischemia/reperfusion. *Biotec Histochem*. 2022; 97: 415–22.

14. Bakirhan EG, Yanilmaz EMB, Tüfekci KK, Bakirhan F, Susam S. Maternal high-fat diet impairs cognitive performance by altering hippocampal GRP78/PERK axis and BDNF expression in adult female rat offspring: the potential protective role of N acetylcysteine. *J Mol Histol.* 2025; 56: 189.
15. Alqahtani S, Mahmoud AM. Gamma-glutamylcysteine ethyl ester protects against cyclophosphamide-induced liver injury and hematologic alterations via upregulation of PPAR $\gamma$  and attenuation of oxidative stress, inflammation, and apoptosis. *Oxid Med Cell Longev.* 2016; 2016: 4016209.
16. Kızılay Z, Erken HA, Çetin NK, et al. Boric acid reduces axonal and myelin damage in experimental sciatic nerve injury. *Neural Regen Res.* 2016;11: 1660–5.
17. Coban FK, Ince S, Kucukkurt I, Demirel HH, Hazman O. Boron attenuates malathion-induced oxidative stress and acetylcholinesterase inhibition in rats. *Drug Chem Toxicol.* 2015; 38: 391–9.
18. Rezaei S, Hosseinimehr SJ, Zargari M, et al. Sinapic acid attenuates cyclophosphamide-induced liver toxicity in mice by modulating oxidative stress, NF- $\kappa$ B, and caspase-3. *Iran J Basic Med Sci.* 2023; 26: 526.
19. Li X, Li B, Jia Y. The hepatoprotective effect of haoqin qingdan decoction against liver injury induced by a chemotherapeutic drug cyclophosphamide. *eCAM.* 2015; 2015: 978219.
20. Caglayan C, Temel Y, Kandemir FM, Yildirim S, Kucukler S. Naringin protects against cyclophosphamide-induced hepatotoxicity and nephrotoxicity through modulation of oxidative stress, inflammation, apoptosis, autophagy, and DNA damage. *ESPR.* 2018; 25: 20968–84.
21. Güler S, Aslaner A, Ellidağ HY, Yildirim Ş, Çakir T. The protective effect of boric acid on cholestatic rat liver ischemia reperfusion injury. *Turk J Med Sci.* 2021; 51: 2716. <https://doi.org/10.3906/SAG-2101-153>.
22. Kahraman E, Göker E. Boric acid exerts anti-cancer effect in poorly differentiated hepatocellular carcinoma cells via inhibition of AKT signaling pathway. *J Trace Elem Medi Biol.* 2022; 73: 127043.
23. Cengiz M, Cetik Yildiz S, Demir C, et al. Hepatopreventive and anti-apoptotic role of boric acid against liver injury induced by cyclophosphamide. *J Trace Elem Med Biol.* 2019; 53: 1–7.
24. Önder Gö, Göktepe Ö, Okur E, et al. Boric acid ameliorates liver injury in rat induced by cyclophosphamide. *Sakarya Med J.* 2023; 13: 210-6.
25. Gündüz E, Yildizhan E, Yaman M, Sen A, Akkus M. Investigation of the protective effect of boric acid against hepatotoxic and nephrotoxic injury induced by acrylamide in rats. *Int J Morphol.* 2023; 41: 368-73.